



HAL
open science

Soliton annihilation into a polychromatic dispersive wave

Alexandre Kudlinski, S. F Wang, Arnaud Mussot, Matteo Conforti

► **To cite this version:**

Alexandre Kudlinski, S. F Wang, Arnaud Mussot, Matteo Conforti. Soliton annihilation into a polychromatic dispersive wave. *Optics Letters*, 2015, 40 (9), pp.2142-2145. 10.1364/OL.40.002142 . hal-02389181

HAL Id: hal-02389181

<https://hal.science/hal-02389181>

Submitted on 2 Dec 2019

HAL is a multi-disciplinary open access archive for the deposit and dissemination of scientific research documents, whether they are published or not. The documents may come from teaching and research institutions in France or abroad, or from public or private research centers.

L'archive ouverte pluridisciplinaire **HAL**, est destinée au dépôt et à la diffusion de documents scientifiques de niveau recherche, publiés ou non, émanant des établissements d'enseignement et de recherche français ou étrangers, des laboratoires publics ou privés.

Soliton annihilation into dispersive waves

A. Kudlinski,^{1,*} S. F. Wang,^{1,2} A. Mussot,¹ and M. Conforti¹

¹*Laboratoire PhLAM, UMR CNRS 8523, IRCICA, USR CNRS 3380,
Université Lille 1, 59655 Villeneuve d'Ascq, France*

²*The Key Lab of Specialty Fiber Optics and Optical Access Network, Shanghai University, 200072 Shanghai, China*

compiled: March 24, 2015

We investigate the propagation of a soliton in an axially-varying optical fiber with a progressive change from anomalous to normal dispersion regimes. Spectral and temporal measurements provide evidence for a complete annihilation of the soliton, which explodes into a polychromatic dispersive wave. This interpretation is confirmed by numerical solution of the generalized nonlinear Schrödinger equation.

OCIS codes: (190.4370) Nonlinear optics, fibers; (190.5530) Pulse propagation and temporal solitons.

The concept of soliton, introduced by Zabusky and Kruskal fifty years ago [1], is of the most impactful and influential discovery of the twentieth century that revolutionized the field of nonlinear physics. A soliton is a special wave that propagates without changing its shape and collides elastically with other wavepackets: it is so a very robust and stable entity. Initially introduced for Korteweg-de Vries equation, it has extended to several other systems (called integrable) [2], encompassing the nonlinear Schrödinger equation (NLSE). However, perturbations can break the integrability of these systems and give rise to phenomena that can even spoil the particle-like nature of solitons, such as their creation and/or annihilation [3–7].

In optical fibers, the integrability breaking of the NLSE can lead to inelastic collisions of orthogonally polarized solitons [10]. Other perturbations, such as intrinsic higher-order dispersion and nonlinearity of optical fibers, also break the integrability [11] and give rise to additional phenomena such as the emission of a dispersive wave (DW) [12, 13] or the soliton self-frequency shift (SSFS) [14]. Combined with these effects, optical fibers with axially-varying dispersion (periodic or not) may also constitute a source of perturbation for solitons. For instance, a single soliton can emit multiple DWs [15–18] or polychromatic DWs [16, 19] as a result of the changing dispersion topography. In all these scenarios, solitons lose more or less energy (into DWs and/or optical phonons) but they continuously adapt their shape so that their solitonic nature is preserved and as a consequence they remain stable. Here we study the effect of a dispersion modulation, obtained by gradually changing the dispersion from anomalous to normal along an axially-varying fiber. A close situation was actually

encountered in Ref. [20], where the authors focused on the soliton blue-shift resulting from a combination third-order dispersion and axially-varying dispersion, but they stopped their investigation at the fiber length where the soliton enters the normal dispersion area. So the behavior of the soliton after this point remains an open question.

In this Letter we show that a soliton progressively going from anomalous to normal dispersion region becomes completely annihilated. It is continuously converted into a polychromatic DW spanning over hundreds of nanometers. This annihilation of the soliton differs by nature from the reversible explosion of dissipative solitons occurring in mode-locked lasers [21–23].

The fiber we used for our experiments was designed to have two zero-dispersion wavelengths (ZDWs) at the input so that a femtosecond pump pulse can excite a fundamental soliton in the anomalous dispersion region located in between the two ZDWs. Then, the idea was to gradually decrease its diameter so that the second (long-wavelength) ZDW progressively decreases and eventually crosses the soliton. At the fiber end, the dispersion at the soliton wavelength would thus be normal. To obtain these properties, we used a photonic crystal fiber (PCF) whose the longitudinal evolution of the diameter is shown in Fig. 1(a). The total length is 8.5 m, and the diameter linearly decreases from 143 to 95 μm over a 1.5 m length. The input pitch Λ is about 1.34 μm and follows the evolution of the outer diameter, the relative hole diameter d/Λ being constant and equal to 0.58 along the fiber. Figure 1(b) shows the group velocity dispersion (GVD) curves at the PCF input (blue) and output (red) calculated with a commercial mode solver (solid lines) and measured with a low-coherence interferometer [24] (full circles). At the PCF input, the GVD is anomalous between 790 and 1465 nm, and the second ZDW decreases almost linearly with fiber length (in the

* Corresponding author: alexandre.kudlinski@univ-lille1.fr

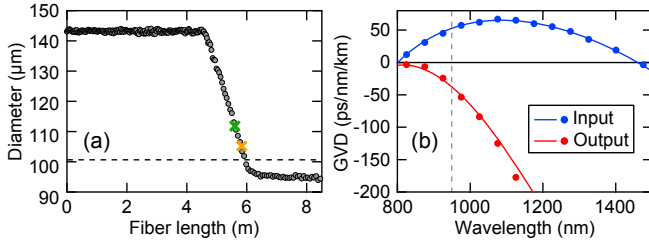


Fig. 1. (a) Longitudinal evolution of the fiber diameter measured during the draw process. The dashed horizontal line depicts the length (diameter) at which the second ZDW disappears and thus dispersion becomes all normal. Green and orange crosses depict the length at which the soliton becomes annihilated for pump peak powers of respectively 110 and 230 W. (b) Calculated (solid lines) and measured (markers) dispersion curves at the fiber input (blue) and output (red). The grey vertical dashed line represents the pump wavelength.

tapered section) until 5.9 m where it reaches 810 nm (see black lines in Fig 2). From this length, the dispersion is all normal over the remaining of the fiber. The nonlinear parameter increases from about 65 to $100 \text{ W}^{-1} \cdot \text{km}^{-1}$ at 950 nm in the tapered section.

In order to excite a fundamental soliton between the the input ZDWs, we launched a gaussian pulse with a full width at half maximum (FWHM) duration of 130 fs, centered at 950 nm. The polarization state of the input field was aligned along a neutral axis of the PCF and the peak power was controlled with a variable attenuator. Figure 2(b) shows the result of a cutback measurement in which the output spectrum was recorded every 0.5 m for a pump peak power of 110 W. The pump pulse excite a fundamental soliton which propagates without experiencing any significant Raman-induced SSFS until 5 m. At this point, the second ZDW (depicted by the black solid line) decreasing due to the tapered section progressively approaches the soliton and eventually crosses it. This results in a dramatic spectral broadening occurring between 5 and 6 m, which will be discussed below. After this length, the whole spectrum spans over about 280 nm at -20 dB (see Fig. 2(a)) and does not evolve anymore with fiber length. These experimental results were confirmed by numerical simulations using the generalized nonlinear Schrödinger equation (GNSLE) including the full dispersion curves, as well as Kerr and Raman nonlinearities. The simulated spectral dynamics, displayed in Fig. 2(c), shows an excellent agreement with the cutback experiment. The dramatic spectral broadening observed at the fiber output is also well reproduced in simulations, as shown by the excellent agreement between experimental (blue line) and simulated (red line) output spectra displayed in Fig. 2(a).

During the cutback experiments, the spectral dynamics was also investigated for a higher pump peak power of 230 W. The corresponding result is shown in Fig. 2(e). In this case, the pump pulse breaks up and excites a fun-

damental soliton which experiences a significant Raman-induced SSFS to reach 1009 nm at 5 m. The energy left in the pump is not high enough to experience any non-linear effect and therefore propagates linearly until the fiber output. The decreasing second ZDW hits the soliton at a length of about 5.5 m causing its spectrum to suddenly broaden very significantly. As in the previous case, the spectrum does not evolve anymore with fiber length from this point. The output spectrum displayed in Fig. 2(d) looks flat (5 dB power variations) from 950 to 1200 nm, and is overall about 330 nm wide (at -20 dB). The simulated spectral dynamics shown in Fig. 2(f) again reproduces the experimental one very accurately, and output spectra (compared in Fig. 2(d)) are also in excellent quantitative agreement.

Let us now focus on the mechanisms causing the spectral explosion of the soliton within the tapered section of the fiber. As can be seen from the spectral dynamics of Fig. 2, the second ZDW (represented by the black solid line) is initially located at 1465 nm, and then decreases almost linearly in the tapered section (from 4.5 to 6 m). At a particular length (depicted by crosses in Fig. 1(a)), it thus gets close enough to the soliton so that the soliton spectrum overlaps the ZDW, which initiates the gener-

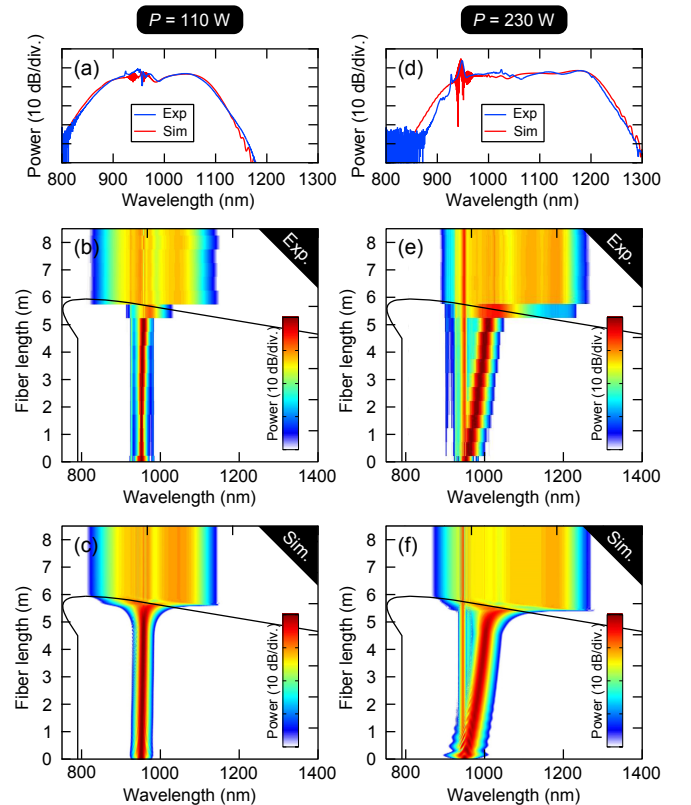


Fig. 2. (a)-(c) Pump peak power of 110 W: (a) Measured (blue line) and simulated (red line) output spectra. (b) Measured and (c) simulated spectral dynamics with fiber length. Black solid lines represent the ZDWs. (d)-(f) Same plots for a pump peak power of 230 W.

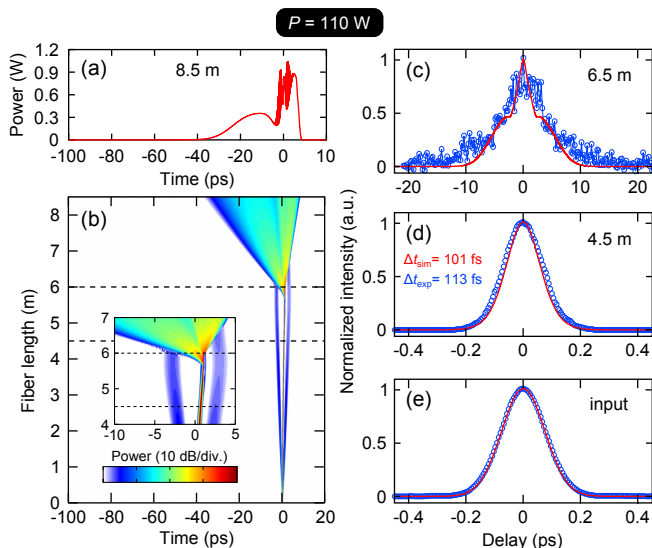


Fig. 3. (a) Simulated output temporal trace for a pump peak power of 110 W. (b) Simulated temporal evolution versus fiber length. Inset: close-up on the tapered section delimited by horizontal dashed lines. (c)-(e) Measured (blue markers) and simulated (red lines) autocorrelation traces at (e) the fiber input, and for fiber lengths of (d) 4.5 m, *i.e.* just before the transition, and (c) 6.5 m, *i.e.* just after the transition.

ation of a DW in the long-wavelength range [25]. This process continuously happens as the ZDW progressively shifts down through the soliton spectrum, which generates DWs at different phase-matching wavelengths, following the process described in [16, 19]. The signature of this process is the broad and smooth spectrum obtained at the fiber output and displayed in Figs. 2(a) and (d). It is indeed composed of many DWs generated at different wavelengths and fiber lengths within the tapered section, which has been termed polychromatic DW [19]. This is especially clear in the simulations of Figs. 2(c) and (f) where one can see that the emission of the long wavelength radiation between 5.5 and 6 m closely follows the evolution of the decreasing second ZDW. Because the soliton spectrum is narrower for the lower pump power of 110 W (7 nm full width at half maximum (FWHM), against 14 nm for 230 W), the emission of the polychromatic DW occurs over a reduced fiber length in the first case, which explains why the output spectrum is narrower (280 nm against 330 nm, respectively).

The temporal analysis of the field along the fiber, represented in Figs. 3 and 4 respectively for pump peak powers of 110 and 230 W, confirms the above interpretation. Let us first discuss the case of the lowest peak power, in which the Raman-induced SSFS is negligible. Figure 3(b) shows the simulated temporal profile versus fiber length, with the inset focusing on the tapered section (delimited by horizontal dashed lines). The right panel shows measured (blue markers) and simulated (red solid lines) autocorrelation traces at the fiber input (Fig. 3(e)), at 4.5 m, *i.e.* just before the start of

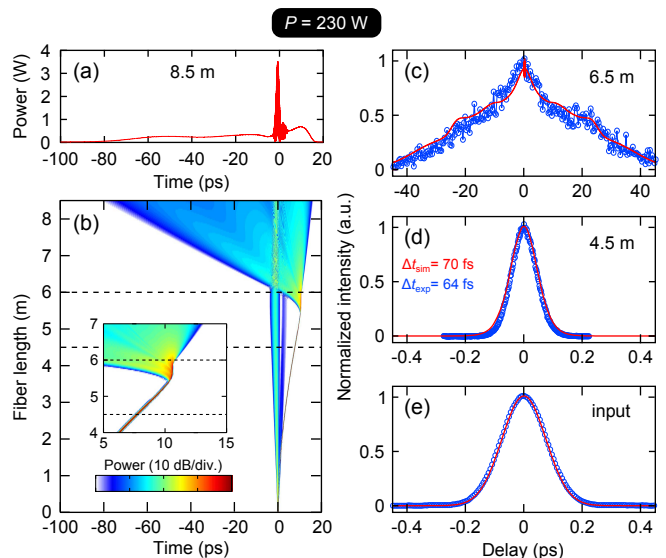


Fig. 4. Same as Fig. 3 for a pump peak power of 230 W.

the transition (Fig. 3(d)), and at 6.5 m, *i.e.* just after the explosion of the soliton (Fig. 3(c)). These figures show that the input gaussian pulse of 130 fs FWHM (Fig. 3(e)) excites a fundamental soliton whose duration at 4.5 m was measured at 113 fs FWHM (against 101 fs in simulations), using an hyperbolic secant profile (Fig. 3(d)). When the second ZDW crosses the soliton at around 5.5 m, the soliton continuously emits a polychromatic DW which rapidly spreads out in time, as can be seen from Fig. 3(b). The simulated output temporal trace plotted in Fig. 3(a) indeed spans over about 40 ps, which is two orders of magnitude longer than the soliton entering the tapered section. The autocorrelation trace of the radiation measured at 6.5 m (just after the second ZDW has crossed the soliton) is represented with markers in Fig. 3(c) and confirms that the soliton has completely exploded into DWs spanning over tens of picoseconds, in good agreement with the simulation result plotted in red line. Autocorrelation traces could not be measured after this point due to the limited scan range of our autocorrelator. The results corresponding to the 230 W pump peak power are shown in Fig. 4 with the same organization as in Fig. 3. In this case, the Raman-induced SSFS is significant and causes a continuous delay of the soliton with regards to the pump residue. It is therefore isolated in both time and spectral domains when it enters the tapered section, which allows its explosion to be very clearly observed (see Fig. 4(b) and its inset). At the tapered section input (4.5 m), its duration was measured at 64 fs (against 70 fs in simulations) as shown from autocorrelation traces of Fig. 4(d). Then, its explosion occurs at 5.5 m, when it crosses the decreasing second ZDW. This results in a massive and progressive temporal broadening until the fiber end, where the output radiation (shown in Fig. 4(a)) spans over more than 100 ps. The peaks located at around 0 on this plot correspond

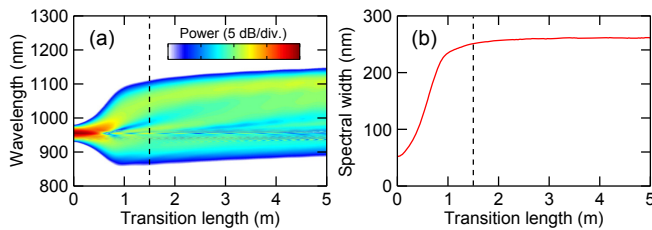


Fig. 5. (a)-(b) Simulated evolution of (a) the output spectrum and (b) the -20 dB spectral width versus length of taper transition for a pump peak power of 110 W.

to the interference of the polychromatic DW with the pump residue. The autocorrelation trace measured just after this soliton annihilation (at 6.5 m) is shown with blue markers in Fig. 4(c). It experimentally confirms that the soliton has been completely transformed into a broad dispersing radiation. Consequently, the spectral and temporal analysis of the output field, both in experiments and simulations of Figs. 2, 3 and 4, shows no trace of the initial soliton which entered the tapered section. The latter has thus been completely annihilated and transformed into DWs (or into a polychromatic DW) thanks to the tapered section of the PCF.

Let us finally emphasize the fact that the configuration we describe here, in which a soliton pulse *progressively* goes from anomalous to normal dispersion, is radically different from launching a soliton *directly* into a normally dispersive medium. In order to illustrate the difference between these two situations and the crucial role of the progressive dispersion change, we plot in Figs. 5(a) and (b) the simulated output spectrum and -20 dB spectral width respectively, as a function of the taper length for a pump peak power of 110 W (corresponding to Figs. 2(a)-(c)). When this length is zero, the spectrum remains almost unaffected because the pulse simply linearly spread out in time due to normal dispersion. For increasing lengths, the spectral width increases until 1 m and does not evolve anymore for longer transitions. Note that the slight red shift of the overall spectrum observed in Fig. 5(a) is due to the fact that the ZDW hits the soliton farther in the fiber and thus at a longer wavelength due to a slight SSFS. The dramatic spectral broadening observed in our configurations (depicted by the dashed vertical line) is the evidence that what we observe is not just a dispersing pulse, but is rather a much more complex and interesting process as discussed above.

To summarize, we have investigated the propagation of a fundamental soliton in a slowly tapered fiber such that it experiences a progressive dispersion sign change from anomalous to normal regime. The spectral and temporal analysis of our experimental and simulation results show that the soliton is progressively annihilated and eventually completely explodes into a polychromatic DW due to the slowly changing dispersion.

We acknowledge R. Habert for the measurement of

dispersion curves. This work was partly supported by the ANR TOPWAVE (ANR-13-JS04-0004) and NoAWE (ANR-14-ACHN-0014) projects, and by the "Fonds Européen de Développement Economique Régional", the Labex CEMPI (ANR-11-LABX-0007) and Equipex FLUX (ANR-11-EQPX-0017) through the "Programme Investissements d'Avenir".

References

- [1] N. J. Zabusky and M. D. Kruskal, Phys. Rev. Lett. **15**, 240 (1965).
- [2] M. A. Ablowitz and P. A. Clarkson, *Solitons, Nonlinear Evolution Equations and Inverse Scattering*, Cambridge University Press (1992).
- [3] C. Au and P. C. W. Fung, Phys. Rev. B **30**, 1797 (1984).
- [4] N. F. Pedersen, M. R. Samuelsen, and D. Welner, Phys. Rev. B **30**, 4057 (1984).
- [5] W. Krolikowski, B. Luther-Davies, C. Denz, and T. Tschudi, Opt. Lett. **23**, 97 (1998).
- [6] V. M. Kranshov, Phys. Rev. B **85**, 134525 (2012).
- [7] M. Onorato, D. Proment, and A. Toffoli, Phys. Rev. Lett. **107**, 184502 (2011).
- [8] M. Onorato, S. Residori, U. Bortolozzo, A. Montina, and F. T. Arecchi, Phys. Rep. **528**, 47 (2013).
- [9] A. Bendahmane, A. Mussot, P. Szriftgiser, O. Zerkak, G. Genty, J. M. Dudley and A. Kudlinski, Opt. Lett. **39**, 4490 (2014).
- [10] B. A. Malomed and S. Wabnitz, Opt. Lett. **16**, 1388 (1991).
- [11] J. N. Elgin, Phys. Rev. A **47**, 4331 (1993).
- [12] P. K. A. Wai, C. R. Menyuk, Y. C. Lee, and H. H. Chen, Opt. Lett. **11**, 464 (1986).
- [13] N. Akhmediev and M. Karlsson, Phys. Rev. A **51**, 2602 (1995).
- [14] F. M. Mitschke and L. F. Mollenauer, Opt. Lett. **11**, 659 (1986).
- [15] F. R. Arteaga-Sierra, C. Milián, I. Torres-Gómez, M. Torres-Cisneros, A. Ferrando, and A. Dávila, Opt. Express **22**, 2451 (2014).
- [16] A. Bendahmane, F. Braud, M. Conforti, B. Barviau, A. Mussot, and A. Kudlinski, Optica **1**, 243 (2014).
- [17] M. Billet, F. Braud, A. Bendahmane, M. Conforti, A. Mussot, and A. Kudlinski, Opt. Express **22**, 25673 (2014).
- [18] M. Conforti, S. Trillo, A. Mussot, and A. Kudlinski, to be published in Sci. Rep., arXiv:1502.02266 (2015).
- [19] C. Milián, A. Ferrando, and D. V. Skryabin, J. Opt. Soc. Am. B **29**, 589 (2012).
- [20] S. P. Stark, A. Podlipensky, and P. S. J. Russell, Phys. Rev. Lett. **106**, 083903 (2011).
- [21] S. T. Cundiff, J. M. Soto-Crespo, and N. Akhmediev, Phys. Rev. Lett. **88**, 073903 (2002).
- [22] S. C. V. Latas and M. F. S. Ferreira, Opt. Lett. **35**, 1771 (2010).
- [23] A. F. J. Runge, N. G. R. Broderick, and M. Erkintalo, Optica **2**, 36 (2015).
- [24] M. Tateda, N. Shibata, and S. Seikai, IEEE J. Quant. Electron. **17**, 404 (1981).
- [25] D. V. Skryabin, F. Luan, J. C. Knight, and P. S. J. Russell, Science **301**, 1705 (2003).

Informational Fifth Page

References

- [1] N. J. Zabusky and M. D. Kruskal, “Interaction of solitons in a collisionless plasma and the recurrence of the initial states,” *Phys. Rev. Lett.* **15**, 240–243 (1965).
- [2] M. A. Ablowitz and P. A. Clarkson, *Solitons, Nonlinear Evolution Equations and Inverse Scattering*, Cambridge University Press (1992).
G. P. Agrawal, *Nonlinear Fiber Optics*, Academic Press (5th edition, 2012).
- [3] C. Au and P. C. W. Fung, *Annihilation and creation of a Korteweg-de Vries Soliton*, *Phys. Rev. B* **30**, 1797 (1984).
- [4] N. F. Pedersen, M. R. Samuelsen, and D. Welner, *Soliton annihilation in the perturbed sine-Gordon system*, *Phys. Rev. B* **30**, 4057 (1984).
- [5] W. Krolikowski, B. Luther-Davies, C. Denz, and T. Tschudi, *Annihilation of photorefractive solitons*, *Opt. Lett.* **23**, 97 (1998).
- [6] V. M. Kranshov, *Radiative annihilation of a soliton and an antisoliton in the coupled sine-Gordon equation*, *Phys. Rev. B* **85**, 134525 (2012).
- [7] M. Onorato, D. Proment, and A. Toffoli, *Triggering Rogue Waves in Opposing Currents*, *Phys. Rev. Lett.* **107**, 184502 (2011).
- [8] M. Onorato, S. Residori, U. Bortolozzo, A. Montina, and F. T. Arecchi, *Rogue waves and their generating mechanisms in different physical contexts*, *Phys. Rep.* **528**, 47 (2013).
- [9] A. Bendahmane, A. Mussot, P. Szriftgiser, O. Zerkak, G. Genty, J. M. Dudley and A. Kudlinski, Experimental dynamics of Akhmediev breathers in a dispersion-varying optical fiber, *Opt. Lett.* **39**, 4490–4493 (2014).
- [10] B. A. Malomed and S. Wabnitz, *Soliton annihilation and fusion from resonant inelastic collisions in birefringent optical fibers*, *Opt. Lett.* **16**, 1388 (1991).
- [11] J. N. Elgin, “Perturbations of optical solitons,” *Phys. Rev. A* **47**, 4331–4341 (1993).
- [12] P. K. A. Wai, C. R. Menyuk, Y. C. Lee, and H. H. Chen, “Nonlinear pulse propagation in the neighborhood of the zero-dispersion wavelength of monomode optical fibers,” *Opt. Lett.* **11**, 464–466 (1986).
- [13] N. Akhmediev and M. Karlsson, “Cherenkov radiation emitted by solitons in optical fibers,” *Phys. Rev. A* **51**, 2602–2607 (1995).
- [14] F. M. Mitschke and L. F. Mollenauer, “Discovery of the soliton self-frequency shift,” *Opt. Lett.* **11**, 659–661 (1986).
- [15] F. R. Arteaga-Sierra, C. Milián, I. Torres-Gómez, M. Torres-Cisneros, A. Ferrando, and A. Dávila, “Multi-peak-spectra generation with cherenkov radiation in a non-uniform single mode fiber,” *Opt. Express* **22**, 2451–2458 (2014).
- [16] A. Bendahmane, F. Braud, M. Conforti, B. Barviau, A. Mussot, and A. Kudlinski, “Dynamics of cascaded resonant radiations in a dispersion-varying optical fiber,” *Optica* **1**, 243–249 (2014).
- [17] M. Billet, F. Braud, A. Bendahmane, M. Conforti, A. Mussot, and A. Kudlinski, “Emission of multiple dispersive waves from a single Raman-shifting soliton in an axially-varying optical fiber,” *Opt. Express* **22**, 25673–25678 (2014).
- [18] M. Conforti, S. Trillo, A. Mussot, and A. Kudlinski, “Parametric excitation of multiple resonant radiations from localized wavepackets,” to be published in *Sci. Rep.*, arXiv:1502.02266 (2015).
- [19] C. Milián, A. Ferrando, and D. V. Skryabin, “Polychromatic Cherenkov radiation and supercontinuum in tapered optical fibers,” *J. Opt. Soc. Am. B* **29**, 589–593 (2012).
- [20] S. P. Stark, A. Podlipensky, and P. S. J. Russell, “Soliton Blueshift in Tapered Photonic Crystal Fibers,” *Phys. Rev. Lett.* **106**, 083903 (2011).
- [21] S. T. Cundiff, J. M. Soto-Crespo, and N. Akhmediev, “Experimental evidence for soliton explosions,” *Phys. Rev. Lett.* **88**, 073903 (2002).
- [22] S. C. V. Latas and M. F. S. Ferreira, “Soliton explosion control by higher-order effects,” *Opt. Lett.* **35**, 1771–1773 (2010).
- [23] A. F. J. Runge, N. G. R. Broderick, and M. Erkintalo, “Observation of soliton explosions in a passively mode-locked fiber laser,” *Optica* **2**, 36–39 (2015).
- [24] M. Tateda, N. Shibata, and S. Seikai, “Interferometric method for chromatic dispersion measurement in a single-mode optical fiber,” *IEEE J. Quant. Electron.* **17**, 404–407 (1981).
- [25] D. V. Skryabin, F. Luan, J. C. Knight, and P. S. J. Russell, “Soliton Self-Frequency Shift Cancellation in Photonic Crystal Fibers,” *Science* **301**, 1705–1708 (2003).